

Analysis of NASA Common Research Model Dynamic Data in JAXA Wind Tunnel Tests

Seigo Koga¹, Masataka Kohzai², Makoto Ueno³, Kazuyuki Nakakita⁴, Norikazu Sudani⁵
Japan Aerospace Exploration Agency, Chofu, Tokyo, 182-8522, Japan

The JAXA 2m x 2m Transonic Wind Tunnel (JTWT) conducted tests for 80% scaled NASA Common Research Model (CRM). The dynamic data including buffet measurement with strain gauges and dynamic pressure sensors were acquired at 50,000 Hz sampling rate. A prediction of buffet phenomenon is one of important factors to design aircraft. If buffet phenomenon occurs, dynamic bending and torsion moment are measured with wing-root strain gauges. Spectrum analyses are being executed for the strain gauges and dynamic pressure data. It is expected to observe dynamic flow separation at points around where the relation with lift coefficient data and pitching moment coefficient is non-linear. This paper describes overview of the tests and the analysis data.

Nomenclature

C_L	=	lift coefficient
C_m	=	pitching moment coefficient
c	=	chord length, m
f	=	frequency, Hz
f_s	=	sampling rate, Hz
f_x	=	cut-off frequency, Hz
M	=	Mach number
L/D_{\max}	=	maximum lift-drag ratio
P_0	=	stagnation pressure, kPa
Re_c	=	Reynolds number based on aerodynamic chord
S_α	=	integral of strain gauge power spectral densities at angle of attack α
U_∞	=	free-stream velocity, m/s
α	=	angle of attack, deg
κ	=	reduced frequency based on chord
η	=	fraction of wing semi-span

I. Introduction

To assess the state-of-the-art computational fluid dynamics (CFD), focusing on drag prediction accuracy, the AIAA Applied Aerodynamics Technical Committee has been holding CFD Drag Prediction Workshops (DPW).¹ The NASA Langley National Transonic Facility (NTF) and the NASA Ames 11-ft wind tunnel have conducted wind tunnel tests on a model called the Common Research Model (CRM) and obtained the force and moment, surface pressure, model deformation, and surface flow visualization data that serve for validation for the CFD results in the fourth Drag Prediction Workshop (DPW-IV).^{2,3}

Japan Aerospace Exploration Agency (JAXA) has been working through the drag prediction with experimental fluid dynamics (EFD) and CFD. The JAXA 2m x 2m Transonic Wind Tunnel (JTWT) planned a set of wind tunnel tests for the CRM and fabricated an 80% scaled NASA CRM model. The tests were conducted and the static and dynamic data were obtained in the tests. The data acquired in the dynamic data measurement included the buffet

¹ Engineer, Wind Tunnel Technology Center, koga.seigo@jaxa.jp, Member AIAA.

² Researcher, Wind Tunnel Technology Center, kohzai.masataka@jaxa.jp, Member AIAA.

³ Associate Senior Researcher, Wind Tunnel Technology Center, ueno.makoto@jaxa.jp, Member AIAA.

⁴ Senior Researcher, Wind Tunnel Technology Center, nakakita.kazuyuki@jaxa.jp, Member AIAA.

⁵ Senior Researcher, Wind Tunnel Technology Center, sudani.norikazu@jaxa.jp, Member AIAA.

measurement data with strain gauges and dynamic pressure data. Buffet phenomenon is one of important factors to design aircraft because irregular flow separation causes the unsteady phenomenon. It is necessary to predict buffet onset for design of aircraft at off-design point. To observe it, the dynamic data are necessary to be acquired at high rate. The data sampling rate in the tests was set up at 50,000Hz. Spectrum analyses are being executed for the strain gauges and dynamic pressure data and characteristic peak frequencies appear at given conditions.

II. Test Overview

A. Facility Description

The JTWT is a closed-circuit and continuously operating facility (Figure 1), which can produce transonic flow ranging from Mach number 0.1 to 1.4. The stagnation pressure can be varied from 50 to 150kPa when only the main blower is used ($M \leq 0.9$) and from 50 to 120kPa when the suction blower is used for more than high subsonic speeds ($M > 0.9$). The stagnation temperature can be controlled in the range of 308 to 333K, and the maximum Reynolds number is 20 million per meter. The size of the test section, which is a cart type, is 2m high and 2m wide. This wind tunnel has been used for measuring aerodynamic characteristics and stability of aircrafts developed in Japan since 1960.

B. Model Description

The size of the model used in the tests is 80% of the NASA CRM model⁴, because the size of the JTWT's test section is 80% of NTF. The picture of the model installed in the test section is shown in Figure 2. The length of the body is 1.355m and the full span is 1.269m. The reference area is 0.179m² and the mean aerodynamic chord is 0.1513m.

C. Measurement System for Dynamic Data

Measurement system to obtain dynamic data consisted as shown in Figure 3 and equipments are arranged as shown in Figure 4.

- 1) Surface static pressure: The model has 325 static pressure taps on the main wing, 33 taps on the horizontal stabilizer, 33 taps on the body, five taps on the support sting surface, 10 taps on the left nacelle surface, five total pressure probes through the left nacelle. Five ESP pressure scanners are mounted inside the forward of the fuselage.
- 2) Model attitude: An accelerometer is installed in the forward of the fuselage to measure the attitude of the model.
- 3) Buffet: 2-axis metallic foil-type strain gauges that can measure strain in X and Y directions are installed at each the wing-roots: one is on upper surface, the other on lower surface for temperature drift reduction. The diameter of the strain gauge is 8mm. Two bridge boxes are mounted inside fuselage. These strain gauges provide main wing bending and torsion data.
- 4) Force and moment: 6-component internal balance attached to a blade support sting is installed inside the fuselage.
- 5) Inertial force: Three 3-axis accelerometers are mounted in the fuselage. Two of them are at the upper right and lower left of fore-body, the other at the upper left of aft-body.
- 6) Dynamic pressure: Kulite Semiconductor Products, Inc.'s dynamic pressure sensors (Kulites) are mounted in both wings. Three are on the upper surface of the left wing and one is on the lower surface of the right wing. The positions of these sensors are shown in Table 1. The pressure range of these Kulites is 10psi differential. The sleeve length is 0.1 inch. The positions of Kulite sensor 2 and 4 are based on the NASA CRM model.

The data acquired in the test were model position, buffet, force and moment, inertial force, and dynamic pressure. In these tests, surface static pressure data was not acquired, because ESP cables could not pass a cavity inside the support sting.

Table 1. Positions of Kulites

No.			x/c	η
1		Inner	0.689	0.701
2	Upper of the left wing	Center	0.639	0.716
3		Outer	0.689	0.731
4	Lower of the right wing		0.612	0.722

D. Test Conditions

The tests for dynamic data were conducted on the condition as shown Table 2. Each height of trip dots of the three patterns, “-”, “N”, “+++”, which was determined based on the method of Braslow et al⁵, is shown in Table 3. In chapter III, the data of strain gauge 1 and Kulite sensor 1 for trip pattern “N” are used for analysis, because the data of the other sensors are insufficiency and it is expected that turbulence transition of flow was occurred under the condition of the trip pattern.

Table 2. Test conditions

P_0	120kPa ($Re_c = 2.27$ million at M0.85)
M	0.70, 0.81, 0.83, 0.85
α	-2 to 7deg
Height of trip dots	3 patterns (“-”, “N”, “+++”)

Table 3. Height of trip dots of three patterns (Unit: in/1000)

Pattern	Assumed stagnation pressure	Inner	Middle	Outer
+++	50kPa	6.5	5.6	5.0
N	100kPa	3.9	3.9	3.5
-	120kPa	3.5	3.1	3.1

III. Data Reduction

The data sampling rate (f_s) in the tests was set up at 50,000Hz, thus, Nyquist frequency was 25,000Hz. 19,000Hz was chosen as the cut-off frequency of filters (f_x) instead of 19,700Hz that is $2.54 f_s$ according to the manual of the filter (NF Corporation’s P-86) setting for using as an anti-aliasing filter due to a specification of the filter setting.

If buffet phenomenon occurs, dynamic bending and torsion moment are measured with wing-root strain gauges. Several spectrum analyses are executed for the strain gauges and dynamic pressure data. It is expected to observe dynamic flow separation around points where the relation with lift coefficient data and pitching moment coefficient is non-linear (Figure 5). Time-series signal data, electric voltage, are converted to a frequency domain spectrum by fast Fourier transformation (FFT) that is one of discrete Fourier transform (DFT). Power spectral density (PSD) is estimated by Welch’s method to smooth data. The plots of PSDs by Welch’s method⁶ of the strain gauge and Kulite sensor data at given angles of attack for M0.85 and M0.70 are shown in Figure 6. The plots, Figure 6 (a) and (b), show that PSDs of both of the strain gauge and sensor increase, as the angle of attack increases from 3.3deg, while Figure 6 (c) and (d) show that PSDs of them increase at the higher angle of attack. Figure 6 (b) indicates a distinct peak of PDS at 169Hz, which is not the modal frequency shown in Figure 7 and described in chapter IV.

Furthermore, PSD is estimated by Yule-Walker Autoregressive (AR) model⁷ that is a parametric method. The left plot of Figure 8 (a) shows the relation of the integral of PSDs (S_a) from 0Hz to the maximum frequency of 25,000Hz to the angle of attack, while the right one shows buffet intensity parameter C_B described by Balakrishna et al.³ The plot of JTWT data indicates the increase of S_a from the angle of attack of around 3deg at M0.83 and M0.85. The onset angle of the S_a increase is a little higher compared with the one of the data of NTF. In addition, the plot of the root-mean-squared (rms) Kulite pressures at given angles of attack is shown in Figure 8 (b). The value increases as the angle of attack increases to 3deg and decreases from 3deg to 4.5deg for M0.85 data. Moreover, the value increases at the higher angles of attack than 4.5deg. The features of the plots almost correspond to the NTF data, while angles of extreme value are higher than the NTF data.

Figure 9 shows contour maps of PSDs data of strain gauge and Kulite sensor with frequencies the horizontal axis and angles of attack on the vertical axis at M0.85, M0.83, M0.81, and M0.70. These figures show that several peaks on the PSDs appear. In both figures of the strain gauge and the Kulite sensor, a spectral density of a particular frequency, 169Hz, increases as the angle of attack increases from 2.5deg to 6deg for M0.85, from 4.5deg to 6.5deg for M0.83. The peaks of 183Hz appear from 3deg to 3.5deg for M0.83 and from 4deg to 6deg for M0.81. On the other hand, it is considered that strong peaks of the strain gauge data in particular at high angles of attack are attributed to modal frequencies of the model and ones of the Kulite sensor data around 300Hz are due to noise of the blower as described in chapter IV. Figure 10 shows contour maps of PSDs for the dynamic balance data at M0.85. Particularly the figures for the drag (F_x), lateral force (F_y), and yawing moment (M_z) data also indicate the peak at 169Hz.

IV. Considerations

One of the causes of the difference between the data of JTWT and NTF as shown in Figure 8 is the different Reynolds number. The slight difference of the Kulite sensor position can also be other matter of the difference in Figure 8 (b). That is because a sensor location is considered to be sensitive for measuring pressures. Figure 11 shows the pictures of oil-flow tests at M0.85 and indicates that the flow around the Kulite sensor position is very variable as the angle of attack changes. Accordingly, it is considered that the particular fluctuating flow starts at around the angle of attack of the maximum lift-drag ratio (L/D_{\max}) and the buffet intensity increases as the angle of attack increases and a flow separation line spreads to nearby wing tip.

Although the peak frequency considered as caused by buffet phenomenon appears around 169Hz, the frequency can correspond to other factors; blower, porous wall, modal frequencies.

- 1) Blower: The Main blower of JTWT is a two-stage axial compressor with 32 rotating blades and 28 stator blades on each stage. The rotation speed was 578-600rpm for M0.85. The peak frequency around 308-320Hz appears to be caused by the blower.
- 2) Porous wall: Distance between holes of the porous wall in a flow direction is 41.57mm and flow speed is 286m/s at M0.85. Hence, the frequency caused by porous wall is assumed to be around 6880Hz.
- 3) Modal frequencies: In no-wind and hammering tests to measure the response of the model after it was subjected to impulse excitation, some modal frequency was detected for strain gauge 1 data (10-12, 18-19, 48-50, 68-70, 145, 153, 182, 325, 350Hz, etc.) and for Kulite sensor 1 data (for example, 50, 150, 250, 400Hz, etc.) as shown in Figure 7.

The peak frequency around 169Hz is not attributed to such factors. That is why the frequency of shock buffet motion can be 169Hz and the buffet onset occurs at around 3deg. Shock oscillation at transonic speed was reported and the reduced frequency $\kappa = 2\pi f/U_\infty$ was described by Lee.^{8,9} Lee proposed a possible mechanism of self-sustained shock oscillation during transonic buffeting with fully separated flow. According to the data acquired at JTWT, κ is 0.37 if shock oscillation frequency is 169Hz.

V. Summary

The dynamic data of 80% scaled NASA Common Research Model (CRM) were acquired at the JAXA 2m x 2m Transonic Wind Tunnel (JTWT). At M0.85, the buffet onset occurs at around 3deg angle of attack and it corresponds to the NTF data. While the features of the analyzed data almost correspond to the NTF data, the changes of the data occur at higher angles of attack, possibly because JTWT runs were performed in 0.25deg P&P and the angles of attack were corrected by the Mokry's method, while NTF runs were performed in a slow continuous sweep, and Reynolds number is different between the JTWT data and the NTF data. In addition, the pictures of oil-flow tests indicate the change of flow with the increasing angle of attack.

Further analyses, for example, calculations of unsteady aerodynamic forces from dynamic balance outputs and inertial forces will be executed and dynamic Pressure Sensitive Paint (PSP) tests are being planned.

Acknowledgments

The authors gratefully acknowledge Ms. Mellissa B. Rivers of NASA Langley Research Center and the staffs for providing useful information. The authors also appreciate the support of JAXA Transonic Wind Tunnel Section and Advance Technology Section in the tests.

References

- ¹Levy, D., Wahls, R., Zickuhr, T., Vassberg, J., Agrawal, S., Pirzadeh, S., and Hensch, M., "Summary of Data from the First AIAA CFD Drag Prediction Workshop," AIAA Paper, 2002-841.
- ²Rivers, M. B. and Dittberner, A., "Experimental Investigations of the NASA Common Research Model in the NASA Langley National Transonic Facility and NASA Ames 11-Ft Transonic Wind Tunnel (Invited)," AIAA Paper, 2011-1126.
- ³Balakrishna, S. and Acheson, M. J., "Analysis of NASA Common Research Model Dynamic Data," AIAA Paper, 2011-1127.
- ⁴Vassberg, J. C., DeHaan, M. A., Rivers, M. S., and Wahls, R. A., "Development of a Common Research Model for Applied CFD Validation Studies," AIAA paper 2008-6919, Aug. 2008.
- ⁵Braslow, A. L., Knox, E. C., "Simplified method for determination of critical height of distributed roughness particles for boundary-layer transition at Mach numbers from 0 to 5," NASA TN-4363, Sep. 1958.
- ⁶Welch, P.D., "The Use of Fast Fourier Transform for the Estimation of Power Spectra: A Method Based on Time Averaging Over Short, Modified Periodograms," *IEEE Transactions on Audio and Electroacoustics*, , Jun.1967.
- ⁷Hamilton, J. D., "Time Series Analysis," Princeton University Press, 1994.
- ⁸Lee, B. H. K., "Oscillatory shock motion caused by transonic shock boundary layer interaction," *AIAA J* 1990;28(5):942-4.
- ⁹Lee, B. H. K., "Self-sustained shock oscillations on airfoils at transonic speeds," *Progress in Aerospace Sciences* 37 (2001) 147-196.

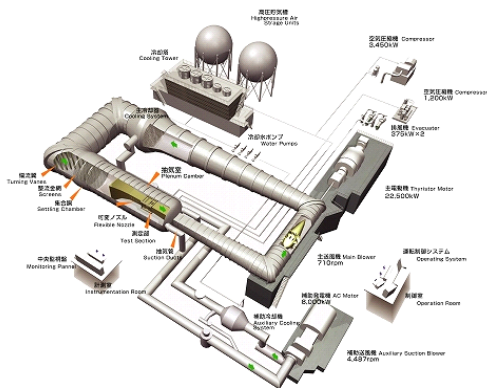


Figure 1. Overall view of JAXA 2m x 2m Transonic Wind Tunnel (JTWT)

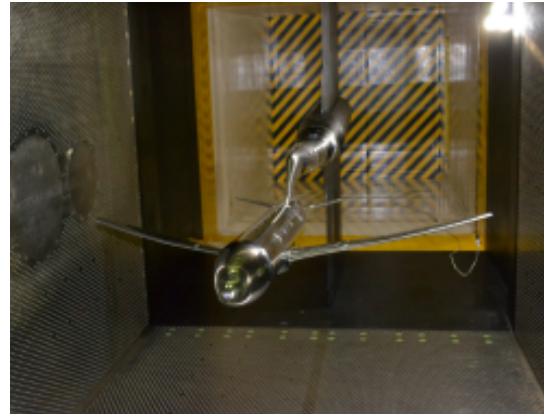


Figure 2. The 80% scaled NASA Common Research Model installed in the JTWT test section

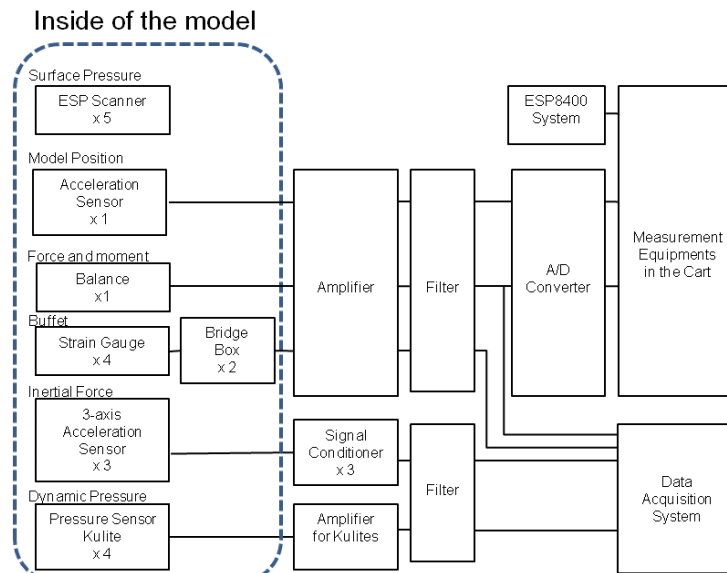


Figure 3. Block diagram of measurement system for dynamic data

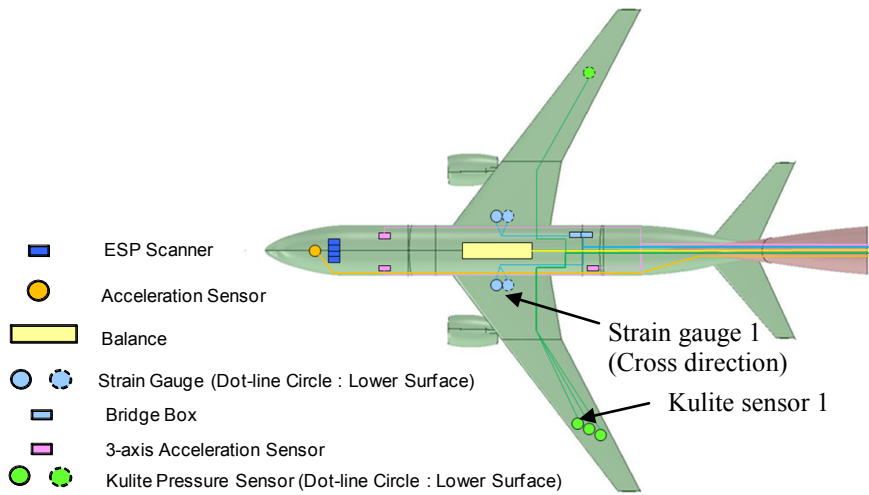


Figure 4. Sketch of configuration of measurement equipments inside the model

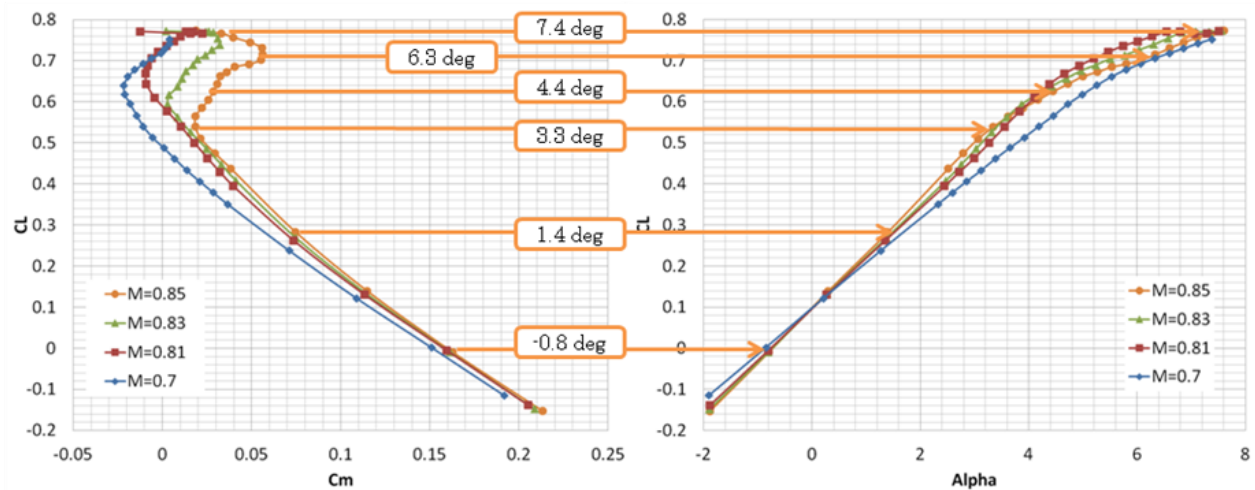


Figure 5. CL vs Cm (left) and CL vs α (right)

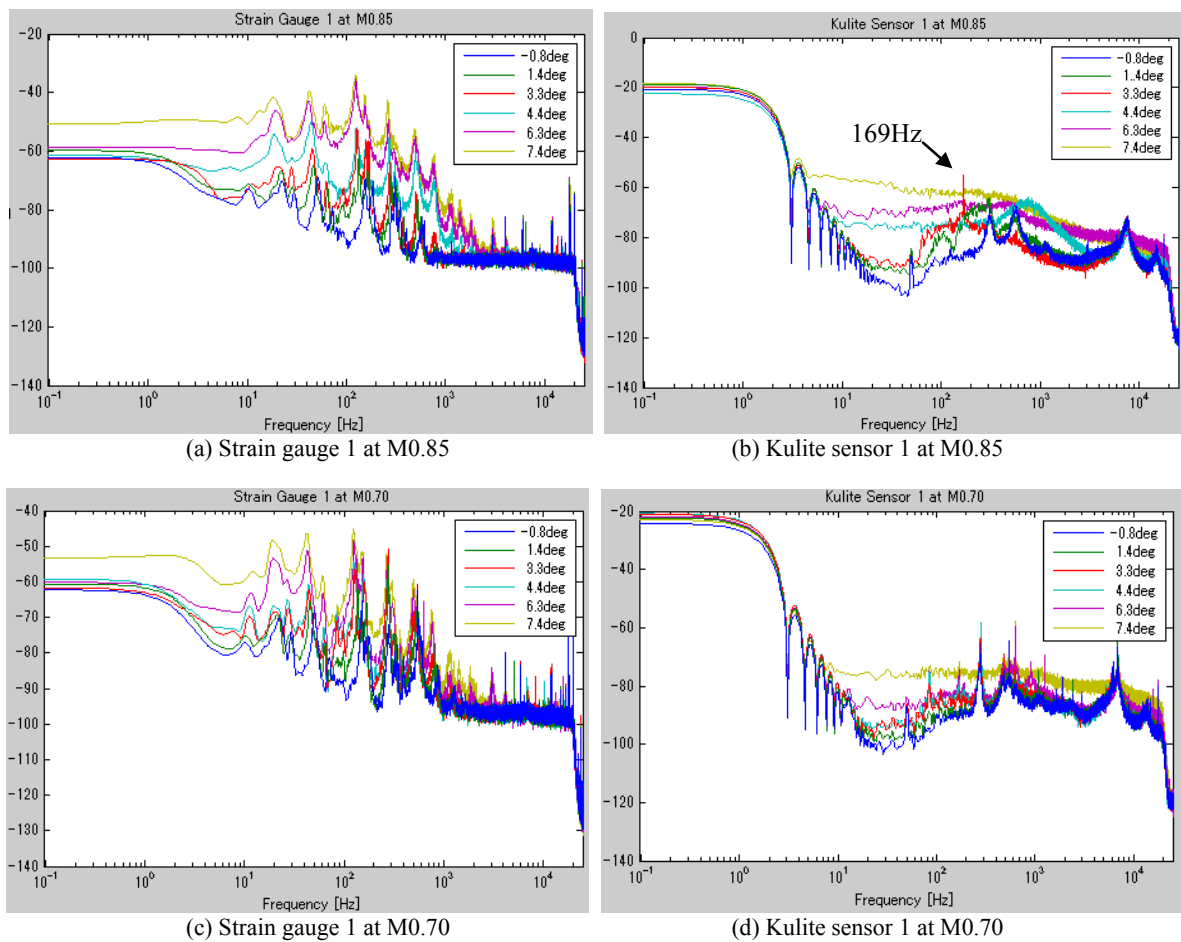


Figure 6. PSDs by Welch's method of the strain gauge 1 (left) and Kulite sensor 1 (right) data

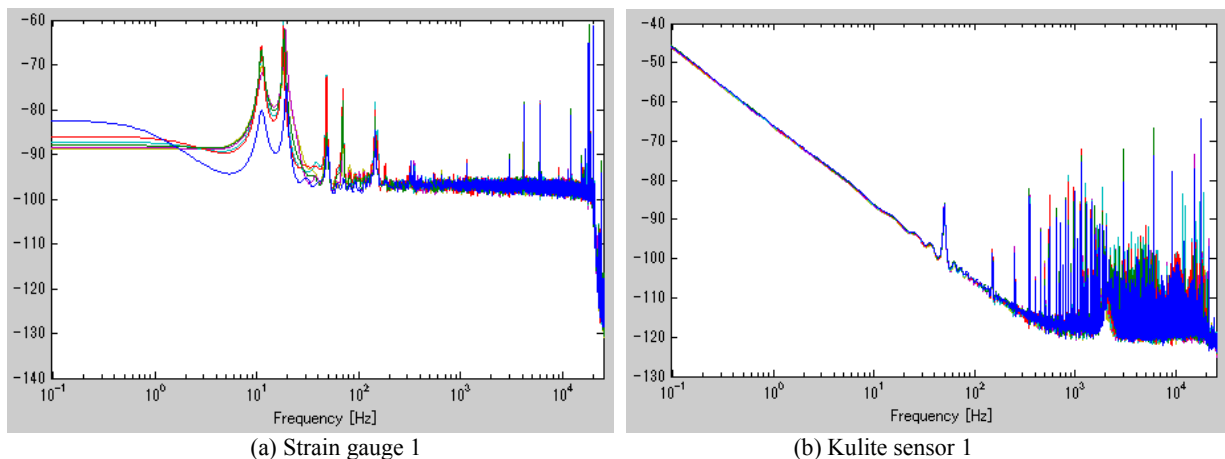


Figure 7. PSDs of no-wind and hammering tests data (left: strain gauge 1, right: Kulite sensor 1)

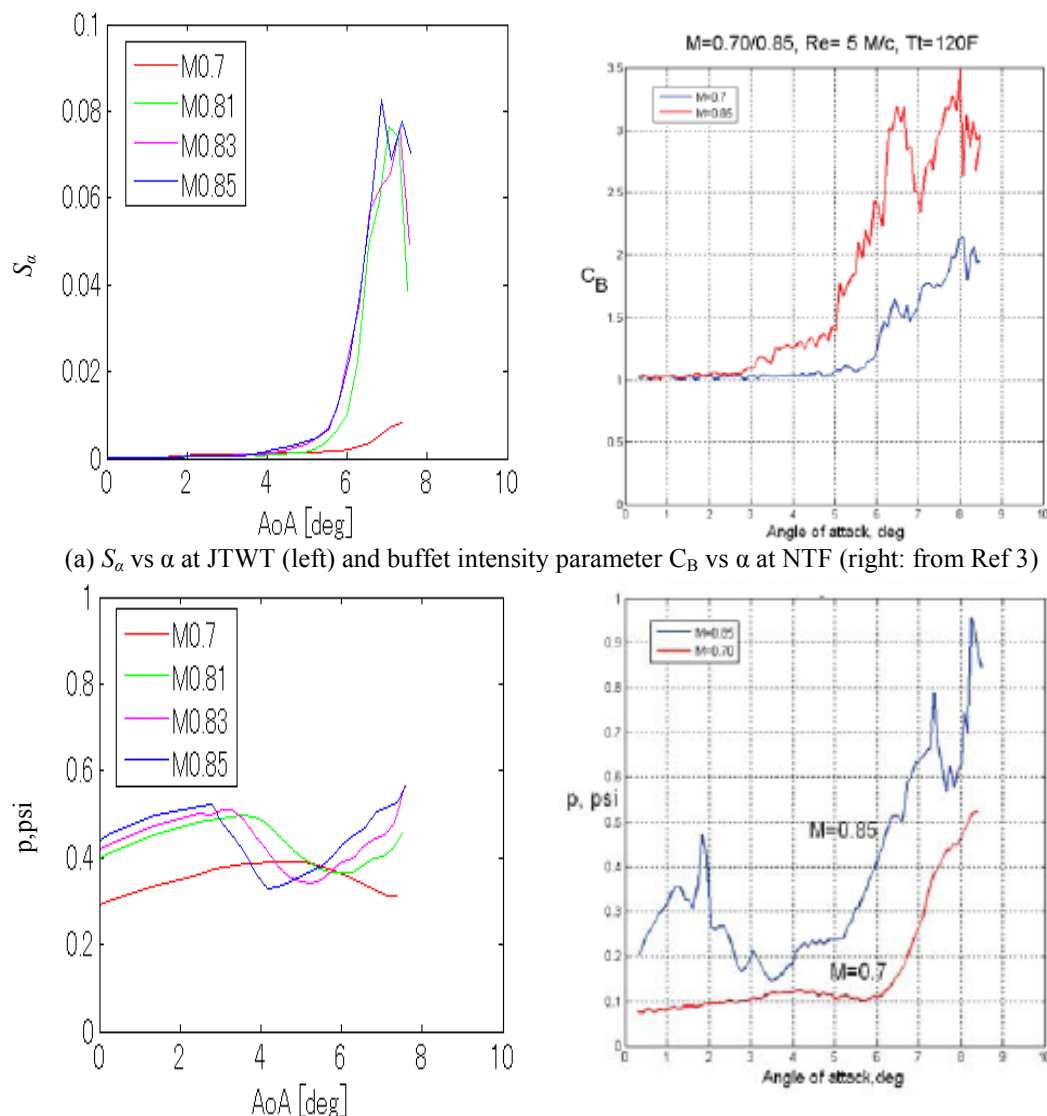


Figure 8. Comparison between the JTWT and NTF data

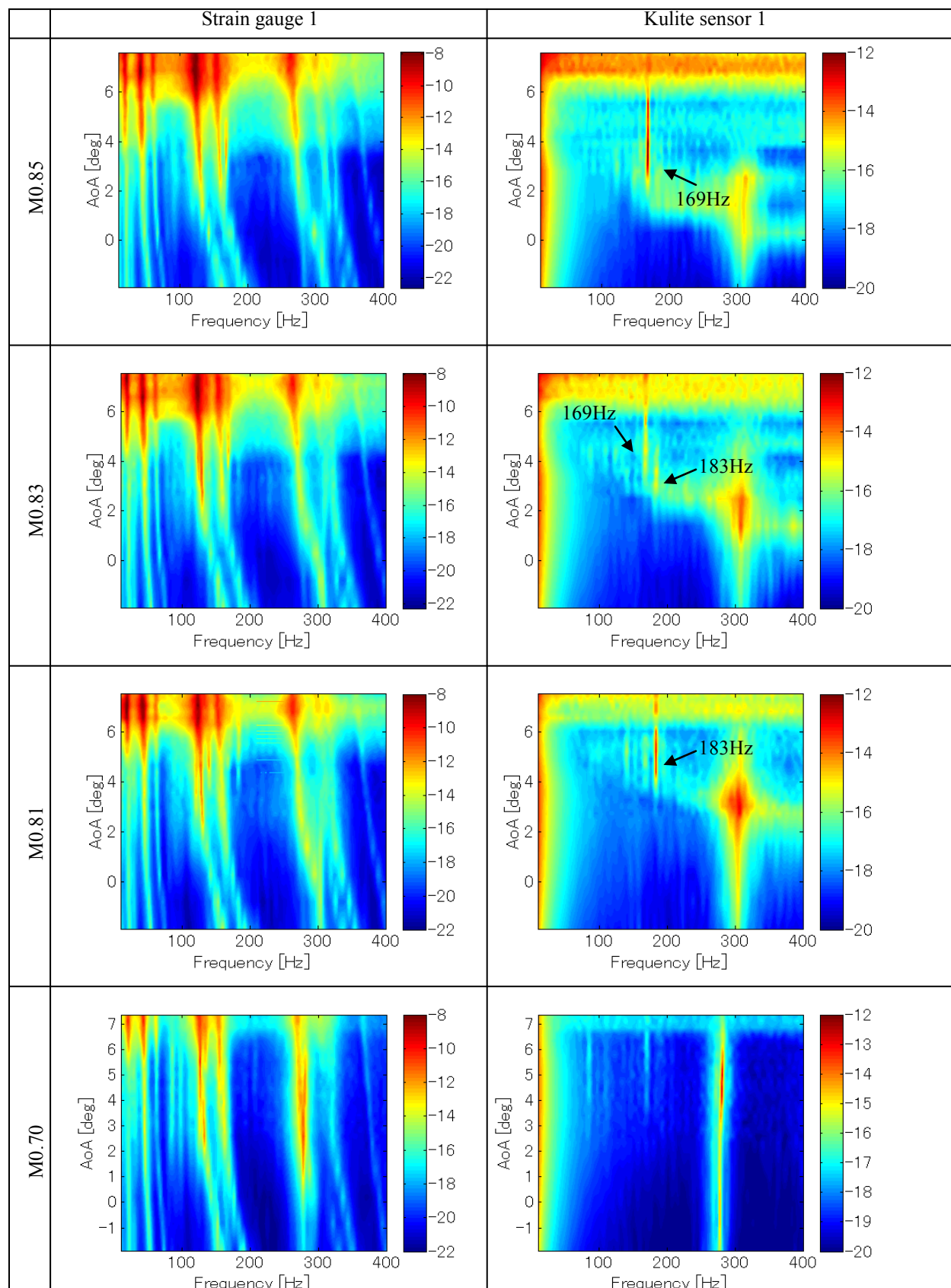


Figure 9. Contour maps of PSDs for strain gauge 1 and Kulite sensor 1 data

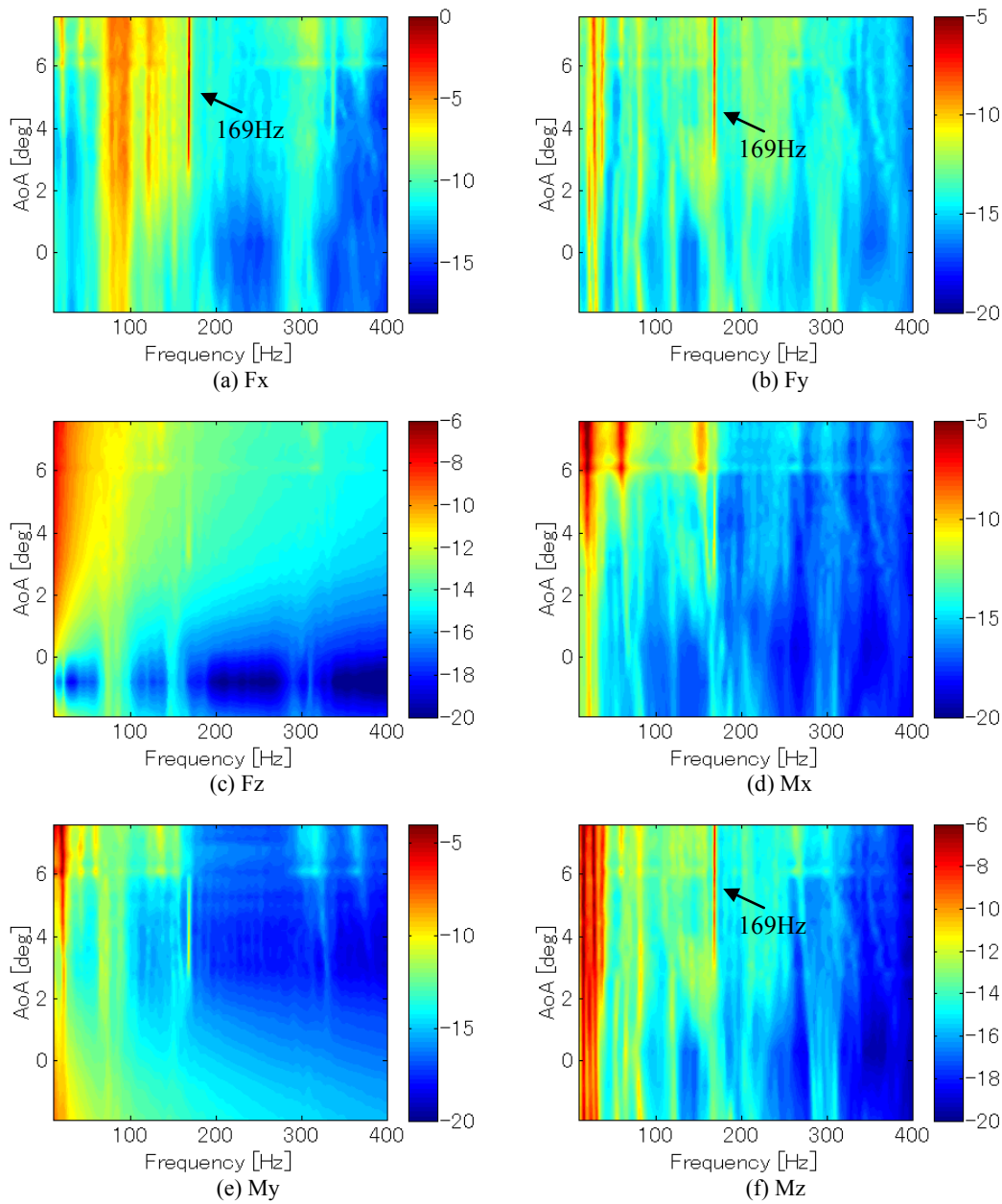


Figure 10. Contour maps of PSDs for the dynamic balance data at M0.85

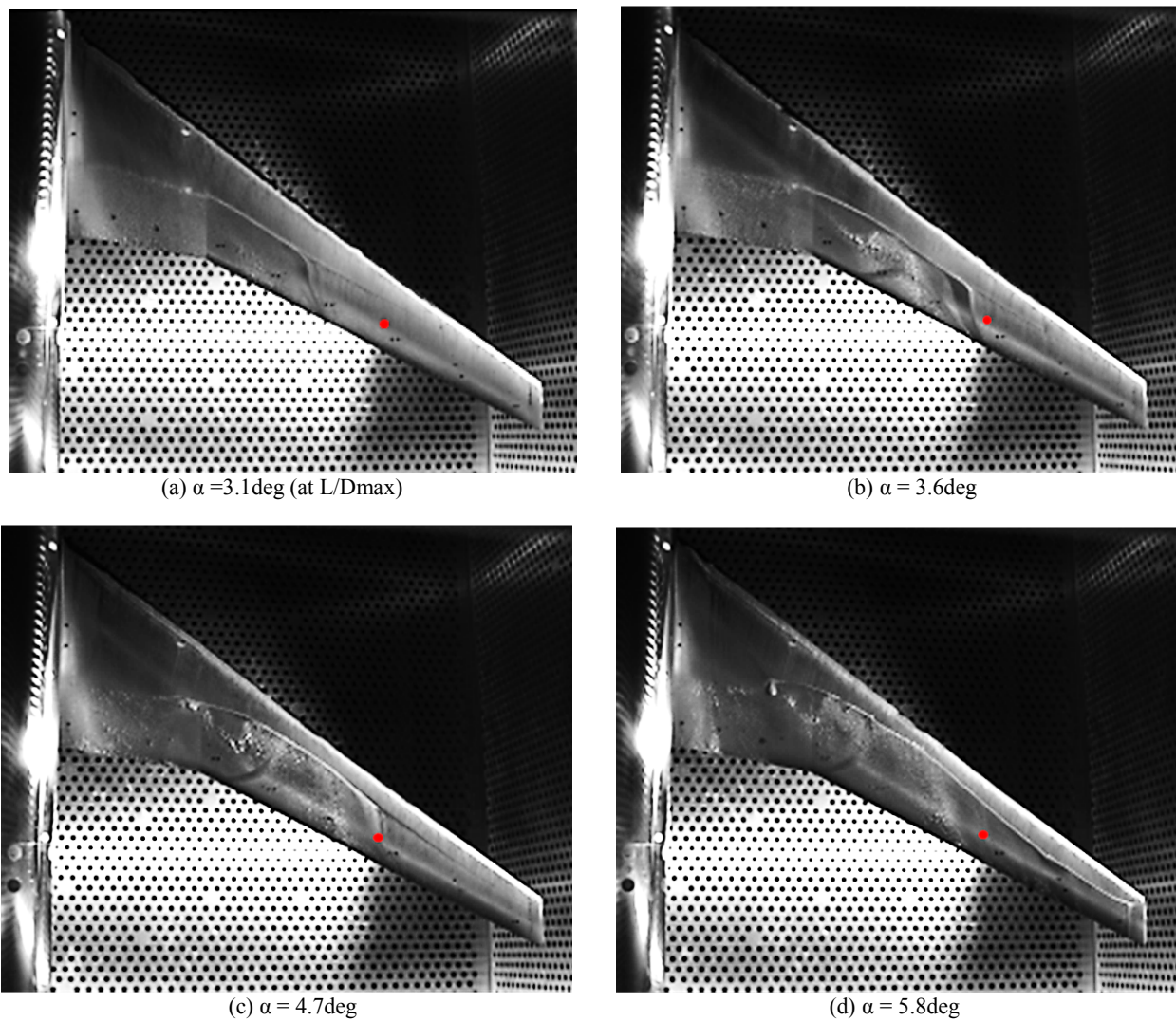


Figure 11. Oil-flow pictures at M0.85 (red dot: symmetric location of Kulite sensor 1)